

This discussion paper is/has been under review for the journal Atmospheric Measurement Techniques (AMT). Please refer to the corresponding final paper in AMT if available.

# Self-Nowcast Model of extreme precipitation events for operational meteorology

G. B. França, M. V. de Almeida, and A. C. Rosette

Federal University of Rio de Janeiro, Rio de Janeiro, Brazil

Received: 19 August 2015 – Accepted: 9 September 2015 – Published: 16 October 2015

Correspondence to: G. B. França (gutemberg@lma.ufrj.br)

Published by Copernicus Publications on behalf of the European Geosciences Union.

10635

## Abstract

Nowadays many social activities require short-term (one to two hours) and local area forecasts of extreme weather. In particular, air traffic systems have been studying how to minimize the impact of meteorological events, such as turbulence, wind shear, ice, and heavy rain, which are related to the presence of convective systems during all flight phases. This paper presents an alternative self-nowcast model, based on neural network techniques, to produce short-term and local-specific forecasts of extreme meteorological events in the area of the landing and take-off region of Galeão, the principal airport in Rio de Janeiro, Brazil. Twelve years of data were used for neural network training and validation. Data are originally from four sources: (1) hourly meteorological observations from surface meteorological stations at five airports distributed around the study area, (2) atmospheric profiles collected twice a day at the meteorological station at Galeão Airport, (3) rain rate data collected from a network of twenty-nine rain gauges in the study area; and (4) lightning data regularly collected by national detection networks. An investigation was done about the capability of a neural network to produce early warning signs – or as a nowcasting tool – for extreme meteorological events. The self-nowcast model was validated using results from six categorical statistics, indicated in parentheses for forecasts of the first, second, and third hours, respectively, namely: proportion correct (0.98, 0.96, and 0.94), bias (1.37, 1.48, and 1.83), probability of detection (0.84, 0.80, and 0.76), false-alarm ratio (0.38, 0.46, and 0.58), and threat score (0.54, 0.47, and 0.37). Possible sources of error related to the validation procedure are discussed. Two key points have been identified in which there is a possibility of error: i.e., subjectivity on the part of the meteorologist making the observation, and a rain gauge measurement error of about 20% depending on wind speed. The latter was better demonstrated when lightning data were included in the validation. The validation showed that the proposed model's performance was quite encouraging for the first and second hours.

10636

## 1 Introduction

Extreme Meteorological Events (EMEs) are frequent in Rio de Janeiro, Brazil and the surrounding area, where they cause considerable damage, such as landslides, floods, loss of human life, and serious delays in landing and take-off procedures at all five airports in the region (see Fig. 1). According to Marengo et al. (2004), an EME is defined as a rare meteorological phenomenon with very low statistical distribution in a particular place. Easterling et al. (2000) defines an EME as an extraordinary event that causes economic and social damage. EMEs were addressed by several authors, e.g., Karl and Easterling (1999); Groisman et al. (1999); Solow (1999); Liebmann et al. (2001); Hegerl et al. (2006), and Alexander et al. (2006), and others. In particular, Teixeira and Satyamurty (2007) studied EME occurrences in southeastern Brazil, using the database from the Center for Weather Forecasting and Climate Studies (CPTEC) and synoptic meteorological observations from the National Institute of Meteorology (INMET). They classified a meteorological event as an EME when rainfall accumulation is higher than one hundred millimeters (mm) in a period of twenty-four hours. EME phases, i.e., initiation, growth, and decay, fall into a nowcasting time scale, implying a short-term forecast. Groisman et al. (2005) presented evidence that the incidence of EMEs has increased about 58% per year in southeastern Brazil since the 1940s. Galeão Airport is located in this region and its flights are significantly affected (by delays and trajectory changes), especially during the landing and take-off phases, by heavy rain, wind shear, and turbulence, which are normally associated with EME incidence. At this airport, a meteorologist generates the nowcast using a conceptual model of how the atmosphere works to extrapolate the location of rainstorms (or other EMEs). This technique is not always suitable since the exact EME stage (i.e., EME initiation, growth, and dissipation) is normally unknown. The present numerical prediction models do not satisfactorily model EMEs in location-specific and short-term scales. Mueller et al. (2003) suggested a nowcast system for storm locations based on fuzzy logic and an atmospheric model. Mass (2012) made a comprehensive review of nowcasting,

10637

including its history, current developments, and future challenges. The objective here is to present an alternative Self-Nowcast Model (SNM) to generate short-term and local-specific predictions of EMEs, based on neural network techniques, for the flight region of Galeão Airport in the city of Rio de Janeiro, Brazil.

## 2 Meteorological data sets and study region

This study used four time series, as follows:

- TEMP represents the upper atmospheric profile for temperature, humidity, wind, and atmospheric pressure, and is collected daily at 00:00 UTC and 12:00 UTC. The radiosonde station used is located at Galeão Airport, whose international aviation code is SBGL, where SB and GL mean Brazil and Galeão, respectively (see Fig. 1). The TEMP time series was obtained online at <http://weather.uwyo.edu/upperair/sounding.html>;
- the Meteorological Terminal Air Report (METAR1), from five meteorological stations (represented by red icons in Fig. 1) in the Rio de Janeiro metropolitan region. The stations (or airports) are Galeão (SBGL), Santa Cruz (SBSC), Santos Dumont (SBRJ), Jacarepaguá (SBJR), and Afonsos (SBAF). METARs are produced hourly; however, SBGL is the only one of the stations that collects atmospheric profiles on a daily basis, together with other pertinent meteorological information in the study area. The data were obtained at the URL address mentioned above;
- rain rate (RR) is obtained from twenty-nine rain gauges (represented by yellow triangles in Fig. 1) distributed around the Rio de Janeiro metropolitan region. The data were obtained at <http://alertario.rio.rj.gov.br/>; and
- lightning reports, regularly collected by the National Integrated Lightning Detection Network (RINDAT), characterize each occurrence by its location (latitude, longitude), intensity polarity (cloud to ground or ground to cloud), and time (UTC)

10638

with accuracy in milliseconds). The data were kindly made available by ELETROBRAS FURNAS Company. These data were only used in the statistical analysis for model validation.

Table 1 summarizes all of the information about time series used for SNM training and validation in this study. Figure 1 shows the study region and the flight region of Galeão Airport.

### 3 Method

Presently, the nowcast at principal Brazilian airports is done by a meteorologist, who uses his experience to integrate different in situ meteorological observations and/or atmospheric model output using conceptual models of how the atmosphere works. The problem with this is the limited time that meteorologists normally have available to integrate all the data and generate a nowcast (Mueller et al., 2003). The idea is to create a self-nowcast model in which a neural network algorithm is used for data fusion, similarly to the work done by Cornman et al. (1998) for detecting and extrapolating weather fronts. At present, one may find applications of neural networks in numerous fields of science, such as modeling, time series investigations, and image pattern recognition, owing to their capability to learn from input data (Haykin, 1999). Figure 2 represents a typical neural network. Normally, stages of neural networks are denoted by a global function as described by Bishop (2006), for example:

$$y_k(\mathbf{X}, \mathbf{W}) = \sigma \left( \sum_{j=0}^M \mathbf{w}_{kj}^{(2)} h \left( \sum_{i=0}^D \mathbf{w}_{ji}^{(1)} x_i \right) \right), \quad (1)$$

where  $\mathbf{W}$  represents all network weights. This global function can be represented in the form of a network diagram (Fig. 2). A neural network is simply a nonlinear function with a set of input and output variables, which are represented by  $x_i$  and  $y_i$ , respectively.

10639

Further details about neural networks and their applications may be found in Pasini et al. (2001); Haykin (1999); Pasero and Moniaci (2004); Bremnes and Michaelides (2007), and Bishop (2006). Figure 3 depicts a general flowchart for the SNM. It has five major steps: (a) extreme meteorological event data processing, (b) definitions of input and output variables, (c) training, (d) validation; and (e) a convergence test having two possible results, i.e., an optimum SNM or retraining. These steps in generating the nowcast are summarized below.

#### 3.1 Data processing

Data processing consisted of three simple tasks. First, the METAR, TEMP, and RR time series were sorted chronologically and their consistency observed, resulting in 63 320 h of meteorological recordings. Second, the rain rate time series, based on  $\text{RR h}^{-1}$ , was used to classify the meteorological recordings into four classes: null, light, moderate, and heavy, for  $0 \leq \text{RR} < 0.2$ ,  $0.2 \leq \text{RR} < 2.4$ ,  $2.4 \leq \text{RR} < 9.9$  and  $\text{RR} \geq 9.9 \text{ mm h}^{-1}$ , respectively.

#### 3.2 Input and output

SNM data fusion is based on a neural network which must be trained; therefore it is necessary to define input and output variables, as described below.

##### 3.2.1 Input variables

These variables are the predictors of the SNM and therefore are responsible for transmitting all atmospheric conditions, including EME phases, to the neural network during its learning process. In Table 1, columns three and four are the primary and derived variables (or predictors), respectively, initially input to the neural network. A meteorological recording is composed of primary and derived variables that are extracted from METAR, TEMP, or RR and calculated using primary variables. The SNM's purpose is to nowcast EMEs; therefore all input (or predictors) should indicate EME phases,

10640

i.e., initialization, growth, and decay. The criterion to select input (primary and derived) variables is based on a conceptual model of how the atmosphere works during an EME, which is characterized by atmospheric instability. For example, the inclusion of input variables as atmospheric instability indices, i.e., K-index (K), Total Totals (TT), and Lapse Rate (LR), and others defined in columns three and four of Table 1 seems quite constructive for the neural network learning process. At the beginning, there were ninety-seven variables. After a simple correlation test, fifty-seven variables remained, divided into twenty-one primary and thirty-six derived variables as listed in columns three and four of Table 1. These variables were initially judged the best data set to transmit atmospheric conditions during neural network training.

### 3.2.2 Output variables

Output is defined as RR, which includes four classes based on RR per hour, numbered as zero, one, two, and three, corresponding to  $0 \leq RR \leq 0.2$ ,  $0.2 < RR \leq 2.4$ ,  $2.4 < RR \leq 9.9$  and  $RR > 9.9 \text{ mm h}^{-1}$ , respectively, as in Table 1, column eight. This output represents the nowcast by the SNM (or neural network algorithm). The latter is responsible for converting the input (or predictors) in the event that all four RR classes occur.

### 3.3 Neural network training

Neural network training is accomplished by trial and error, represented by the SNM looping in Fig. 3. It requires previous knowledge of the phenomenon in conjunction with the experience of the training team. EMEs are characterized by thermodynamic atmospheric patterns represented by local meteorological recordings. In order to carry out the training, the meteorological recording data set was randomly divided into two subsets, i.e., one for training and the other for validating the SNM, corresponding to 70 %, or 44 324 recordings, shown in Fig. 4a and 30 %, or 18 996 recordings, shown in Fig. 4b of the data population. Knowing that the EME forecast problem requires

10641

categorical output, it was decided to use probabilistic neural networks, as suggested by Specht (1990, 1991). The EME is defined as a nowcast corresponding to “yes = class three ( $RR > 9.9 \text{ mm h}^{-1}$ )” or “no = class one, two, or three”.

### 3.4 Validation and other procedure steps

This step consists of comparing SNM forecasts (or output) to one of three true observation conditions, namely: (a) weather conditions (class three of Table 2) reported by METAR, and/or (b) a rain rate higher than  $9.9 \text{ mm h}^{-1}$  reported by at least one rain gauge in the network, and/or (c) lightning reported inside a fifty-kilometer (km) radius centered at Galeão Airport during a one-hour period. The lightning data series was only used for validation purposes. There is a possibility of all three conditions occurring simultaneously. The main reasons for including three different sources of comparison vs. the SNM forecast are: (a) the forecasts represent RR for one, two, and three hours; however, it is well known that rainfall varies highly in time and space and sometimes is not properly registered by rain gauges. Accordingly to Lanza and Vuerich (2009), the error rate associated with rain gauges could be as much as 20 % depending on the wind speed at the gauge edge during rainfall, (b) weather conditions reported in a METAR represent an observation by the meteorologist in an instant of time (ten minutes before the hour); therefore, sometimes it does not correctly represent an entire one-hour period, which is the minimum time interval for an SNM forecast, and (c) the lightning data will be continuously generated during the entire SNM forecast time. Its capability to identify lightning locations (the location error is about five hundred meters in the studied area) beyond the METAR observation depends on the meteorologist's observation skill. The lightning data allows for spreading out the SNM forecast verification to encompass the entire flight area of the Galeão Airport. Following the workflow in Fig. 3, when the validation criteria (e.g., values for statistics) are satisfied, optimum SNM configurations will be obtained. Otherwise, trial and error looping will continue modifying the training data set or number of input variables. The SNM training process is discussed in the next section. The validation criterion is the comparison of EME

10642

forecasts and true observations using a two-dimensional contingency table, which allows the calculation of five categorical statistics used to verify the frequency of correct and incorrect forecasted values, as follows: (1) proportion correct (PC), which shows the frequency of the SNM forecasts that were correct (a perfect score equals one), (2) bias, which represents the ratio between the frequency of SNM estimated events and the frequency of SNM observed events (a perfect score equals one), (3) probability of detection (POD), which represents the probability of those occasions where the forecast event really occurred (hits). The scale varies from zero to one, where one indicates a perfect forecast, (4) false-alarm ratio (FAR), which indicates the fraction of SNM-predicted EMEs that did not occur (a perfect score equals zero), and (5) threat score (TS), which indicates how the SNM forecasts correspond to the observed EMEs (a perfect score equals one). In particular, the TS is relatively sensitive to the climatology of the studied event, tending to produce poorer scores for rare events such as, for example, an EME. Therefore the model is considered optimum when it creates EME nowcasting with scores as near perfect as possible for the five statistics described (Wilks, 2006).

## 4 Analysis and results

In order to assess the performance of the nowcasting system proposed for the flight region of Galeão Airport in Rio de Janeiro, the SNM output variables were divided into four event classes based on RR, namely: class zero: no significant weather; class one: light RR; class two: moderate RR, and class three: EME. Figure 4a and d depicts the classes' frequency in training and validation data sets, respectively, corresponding to 70 and 30 % of the total number of meteorological recordings. It may be observed that class frequencies are not proportionally distributed. In particular, class three (defined as EME) is poorly represented, accounting for about two percent of all meteorological recordings. The latter makes the neural network learning process harder, as that requires – for phenomenon knowledge – a better representation of target class three in

10643

the training data set, i.e. class three should have higher weight than other classes, or at least a similar weight to other classes, in the training data set in order to allow for better neural network training. The next paragraphs present detailed information about the neural network training strategies that were used, attempting to compensate for the low frequency of EME events in the studied data set.

### 4.1 Neural network training

Neural network training is a time-consuming activity. A common strategy is to modify the training data set, for example, taking the original data as a reference to artificially create other new training data sets by modifying the classes' representation in the data population, and/or gradually decreasing input variables by evaluating a particular variable relevance (or contribution) for output results. There is no straightforward set of calculations to accomplish this goal. It is important to mention that the validation data set shown in Fig. 4d has similar class frequencies to the original training data set, shown in Fig. 4a. The idea is to input real scenarios of rare events during the validation process. Table 3 gives information about training strategies used during the first, second, and optimum training sequences. These training strategies are discussed below.

#### 4.1.1 First training

Table 3 helps in understanding the results of the training strategies showing that the first training strategy assumes the following conditions: (a) the starting number of the meteorological recordings is 43 638, (b) the training data set was gradually decreased by reducing recordings from classes zero, one, and two, and the number of recordings in class three was kept constant during each looping step in Fig. 3, (c) the input variables a constant equal to correspond sum of primary and derived variables in columns 3 and 4 of Table 1, (d) the validation are weather condition observations (represented by class in Table 2) in METAR code and/or  $RR > 9.9 \text{ mm h}^{-1}$  (registered by one of the

10644

rain gauge networks), and (e) the model convergence is when statistics parameters are kept unaltered in next looping step as in Fig. 3. Table 3 (training) the neural network converged when the number of meteorological recordings was 22 498 (or about 52% of the total training recordings). Excepting PC, the other statistic results show that neural network were not capable learn much how to forecast EMEs for period of one, two  
 5 three hours. This could be qualified to: (a) the low frequency of class three vs. the other classes, not allowing enough knowledge about EME phases (i.e., initialization, growth and decay) to be transmitted as required, and (b) possibly an inappropriate number of input variables.

#### 10 4.1.2 Second training

Figure 4b shows the class frequency of the initial data set. It demonstrates that the percentage of the EME class (class three) seems slightly better represented than in previous training. Generally speaking, it can be observed from Table 3 that PC remained similar to the first training results, FAR increased and bias, POD and TS were  
 15 slightly enhanced, which possibly means that the SNM learning process had improved somewhat, but not enough. In other words, it appears that this training strategy is proceeding in the right direction.

#### 4.1.3 Optimum SNM training

Table 3 presents the training strategy and tries to give an idea about successive trainings used in the present study. In particular, line three presents the training strategy that produced optimum results. The strategy that was used is similar to the previous trainings apart from the number of input variables, which was previously kept constant; here, the input variables decreased for each looping step in Fig. 2 by taking out the variables with low representativeness for the neural network results. Based on the possibility that heavy rain could occur without simultaneous lightning and vice-versa, the validation statistics results were achieved by two options: first, by considering items  
 20 25

10645

(a) and (b), and second, by considering items (a), (b) and (c) of Sect. 3.4, respectively. The latter item (item c) shows that lightning occurrences, reported inside a radius of fifty kilometers centered at SBGL, represent an EME. Table 3, line four, shows categorical statistical verifications of the optimum model results. The SNM forecast performance  
 5 slowly declines from the first to the second hour and declines more rapidly from the second to the third hour. By including the lightning ( $L$ ) data in the validation, the SNM results were improved, as shown by the first<sup>(L)</sup>, second<sup>(L)</sup>, and third<sup>(L)</sup> hours (as in Table 3, lines eight, ten, and twelve). The comparison between the two validation data sets (with and without lightning data) shows that bias, POD, and FAR values improved  
 10 by 19, 11, and 25% (for the first, second, and third hours); 5, 3, and 6% (for the first, second, and third hours) and 11, 5, and 8% (for the first, second, and third hours), respectively. In particular, the bias values improved more than the other statistics as a result of the inclusion of the lightning data in the validation. In addition, although TS is tending to produce poorer scores for rare events, in here, his results have also improved with the inclusion of lightning data in the validation of optimum training as in  
 15 Table 3, column thirteen. The best SNM result corresponds to the first hour. The bias is the lowest, equal to 1.37 (which means that the results slightly overestimated the observations for the considered forecasts); however, the readings for PC, POD, FAR, and TS are quite respectable, equal to 0.84, 0.38, 0.01, and 0.54, respectively. The results of the SNM for the second hour are slightly less useful than for the first hour forecast, but still acceptable. On the other hand, the statistical values for the third hour forecast are poorer than those for the second hour. One cause of the SNM's overall performance degeneration is that a neural network is a statistical model rather than a physical one, which means that the physical aspects are not included. In summary, it  
 20 25 is possible to state that an optimum SNM should be able to forecast strong atmospheric instability in the study area for up to two hours.

10646

## 4.2 Possible sources of error in the SNM validation

The SNM optimum model output is considered a hit when it corresponds to event observations, if at least one of the following two weather conditions is satisfied, i.e., (1) weather conditions (it is class three in Table 2. In particular, this information is obtained from a human observer and may have some inconsistencies. The latter is common in meteorological observations, thus, consciousness of such matters is important when interpreting results) from METAR at a specific time; and/or (2)  $RR > 9.9 \text{ mm h}^{-1}$  (registered by one of the rain gauge networks). The SNM results are slightly biased as previously presented; therefore, in an attempt to explain that bias, the study pursued an investigation of possible sources of error in the meteorological observations used to verify the model forecasts. First of all, as far as the learning process was concerned, the training data set was composed only of meteorological records with a unique true association between their output (as class three and/or  $RR > 9.9 \text{ mm h}^{-1}$ ) and input variables (representing the thermodynamic atmospheric pattern of an EME from the 15 METAR records, and derived variables). In other words, the training used only meteorological recordings whose output was characterized as true EME. However, in the validation data set, there is a large number of meteorological records where such a unique association (one-to-one relationship between input and output) is not always true; i.e., some meteorological records have a typical thermodynamic pattern of EME (input), but the weather condition (output) does not correspond to an EME (or prevailing actual weather situation). These records were used in the present study to verify SNM forecasts and have consequently produced the results in Table 3. Possible reasons for false alarms and consequently biased SNM results are: (1) hourly METAR records represent quasi-instantaneous meteorological observations (these take about ten minutes to be generated and may carry inconsistencies); therefore the weather condition (output) may be affected by a certain amount of subjectivity on the part of the meteorologist (see discussion below and results in Table 4), and (2) errors associated with the rain gauges, which can be up to 20 % depending on the wind speed. The SNM results for

10647

the first hour which were classified as false alarms were those whose RR was higher than  $8.0 \text{ mm h}^{-1}$  and lower than  $9.9 \text{ mm h}^{-1}$ , representing a maximum SNM error below 10 % for the RR threshold of EMEs ( $RR > 9.9 \text{ mm h}^{-1}$ ). Such a number of false alarms produced by the SNM could easily be attributed to rain gauge measurement error, and (3) isolated heavy rain events causing serious material damage during the summertime, but that were not always registered by the rain gauge network or even by the METAR, since such conditions are not always observed by meteorologists. One example of this would be where the input represents an EME and the output does not; consequently, such a situation may be one of the causes of the biased results obtained in this study. Finally, the comparisons between SNM forecasts and lightning detection have slightly improved all statistical values. These results have provided plenty of evidence that the validation parameters (i.e., RR and class three in Table 2) are not totally appropriated for the SNM validation, so some errors are certainly being introduced into the SNM results; consequently, the actual optimum SNM statistics may be even better than those shown in Table 3.

## 4.3 Study case

Attempting to elucidate the above discussion, this section shows the SNM results for an EME event that occurred from 16:00 to 23:00 (LT) on 18 March 2009. Figure 5 depicts a synoptic weather situation through an enhanced GOES-10 (channel 4) satellite image at 18:00 (LT), where a cloud (or cloud complex) is classified, by an automatic stretch process, as convective (or EME) if its top temperature is lower than  $-30^\circ\text{C}$ . The red box roughly represents the flight region of Galeão Airport in Rio de Janeiro which is influenced by EMEs (located approximately at the center of the red box) and where a complex convective cloud (with cloud top temperature equal to  $-70^\circ\text{C}$ ) is clearly observed in the east. On this day, the K, TT, and LR index values, calculated from the SBGL atmospheric profile, were equal to 33.64, 44.97, and 5.5, respectively, indicating that a typical atmospheric instability pattern was dominating the region. Table 4 shows a comparison between SNM forecasts (column four) and the weather observations

10648

made by the meteorologist and registered in the METAR (columns two and three) for the studied period. From this result, it seems that the SNM overestimated the possibility of an EME (compare columns three and four). However, the problem of verification of the output of the SNM is difficult, since the meteorologist's observation does not always  
5 give a more appropriate weather condition (or a prevailing condition) to be compared with it; therefore, biased results may be obtained from the SNM. Lightning has been coincidentally detected (column five) for all SNM forecasts of EMEs during the time period of this particular case study, which indicates an unstable atmospheric pattern in the flight area of the airport influenced by the event. There is quite strong evidence from  
10 previous analysis that the bias results in Table 3, line three, are unreliable and would certainly be very much lower if appropriate or steady output was used in SNM verification. In summary, the SNM forecasts have usually captured the signs of an atmospheric instability pattern.

## 5 Conclusions

15 Numerical prediction models have demonstrated certain difficulties in attempting to forecast the local or short-term heavy rain, strong wind, and turbulence that are normally associated with EME occurrences. Hence, this study presents an alternative self-nowcast model for short-term and local-specific forecasting of EMEs based on a neural network technique for the flight region of the Galeão's Airport. The main findings of this  
20 study are summarized as follows:

a. the optimum SNM results of EME forecasts for the first and second hours are encouraging, since the categorical statistical values are quite acceptable. The proposed model has a very low computational cost and it is also possible to state that the SNM could alternatively forecast short-term strong atmospheric instability  
25 for the flight region of the Galeão's Airport;

10649

- b. the third hour SNM forecast is biased (best bias is 1.83); perhaps the main reason of such SNM performance degeneration in time is that the neural network model is purely statistical rather than physical, and its use should therefore be limited to short-term nowcasting, possibly up to a two-hour time,
- 5 c. there is visible evidence that the validation data contain a certain amount of uncertainty. Three key considerations about the SNM results vs. validation data and possible sources of error should be addressed. First, the use of METAR weather conditions is affected by subjectivity on the part of the meteorologist and sometimes does not represent prevailing weather conditions. Second, rain gauges used  
10 for data verification can have an error of about 20 % depending on the wind speed. The results showed that SNM forecasts might falsely be classified as hits due to possible rain gauge error. Third, isolated heavy rain events sometimes are not registered by the rain gauge and can contribute to biased SNM results; and
- 15 d. the inclusion of lightning data in the validation significantly improved the SNM statistic results and also provided evidence that weather conditions discussed in the previous item are not totally appropriate for the SNM validation. Finally, the study may conclude that the optimum SNM developed here is clearly capable of predicting signs of a local atmospheric instability pattern in the flight region of  
20 Galeão Airport. Future studies are planned which will include other data sources in the learning process, such as meteorological satellites, RADAR, and SODAR wind profiles.

*Acknowledgements.* The authors thank the Meteorology Program at Federal University of Rio de Janeiro for supporting this work.

## References

- 25 Alexander, L., Zhang, X., Peterson, T., Caesar, J., Gleason, B., Klein Tank, A., Haylock, M., Collins, D., Trewin, B., Rahimzadeh, F., Rahimzadeh, F., Tagipour, A., Rupa Kumar, K.,  
10650



- Revadekar, J., Griffiths, G., Vincent, L., Stephenson, D. B., Burn, J., Aguilar, E., Brunet, M., Taylor, M., New, M., Zhai, P., Rusticucci, M., and Vazquez-Aguirre, J. L.: Global observed changes in daily climate extremes of temperature and precipitation, *J. Geophys. Res.-Atmos.*, 111, D05109, doi:10.1029/2005JD006290, 2006. 10637
- 5 Bishop, C. M.: *Pattern Recognition and Machine Learning*, Springer, New York, NY, USA, 227–229, 2006. 10639, 10640
- Bremnes, J. B. and Michaelides, S. C.: Probabilistic visibility forecasting using neural networks, *Pure Appl. Geophys.*, 164, 1365–1381, 2007. 10640
- Cornman, L. B., Goodrich, R. K., Morse, C. S., and Ecklund, W. L.: A fuzzy logic method for improved moment estimation from Doppler spectra, *J. Atmos. Ocean. Tech.*, 15, 1287–1305, 1998. 10639
- 10 Easterling, D. R., Meehl, G. A., Parmesan, C., Changnon, S. A., Karl, T. R., and Mearns, L. O.: Climate extremes: observations, modeling, and impacts, *Science*, 289, 2068–2074, 2000. 10637
- 15 Groisman, P. Y., Karl, T. R., Easterling, D. R., Knight, R. W., Jamason, P. F., Hennessy, K. J., Suppiah, R., Page, C. M., Wibig, J., Fortuniak, K., Razuvaev, V. N., Douglas, A., Førland, E., and Zhai, P.-M.: Changes in the probability of heavy precipitation: important indicators of climatic change, *Climatic Change*, 42, 243–283, 1999. 10637
- Groisman, P. Y., Knight, R. W., Easterling, D. R., Karl, T. R., Hegerl, G. C., and Razuvaev, V. N.: Trends in intense precipitation in the climate record, *J. Climate*, 18, 1326–1350, 2005. 10637
- 20 Haykin, S.: *Neural Networks: A Comprehensive Foundation*, Prentice Hall New Jersey, New Jersey, USA, 1–24, 1999. 10639, 10640
- Hegerl, G. C., Karl, T. R., Allen, M., Bindoff, N. L., Gillett, N., Karoly, D., Zhang, X., and Zwiers, F.: Climate change detection and attribution: beyond mean temperature signals, *J. Climate*, 19, 5058–5077, 2006. 10637
- 25 Karl, T. R. and Easterling, D. R.: Climate extremes: selected review and future research directions, in: *Weather and Climate Extremes*, Springer, the Netherlands, 309–325, 1999. 10637
- Lanza, L. G. and Vuerich, E.: The WMO field intercomparison of rain intensity gauges, instruments and observing methods, *Atmos. Res.*, 94, 534–543, 2009. 10642
- 30 Liebmann, B., Jones, C., and de Carvalho, L. M.: Interannual variability of daily extreme precipitation events in the state of Sao Paulo, Brazil, *J. Climate*, 14, 208–218, 2001. 10637

10651

- Marengo, J. A., Soares, W. R., Saulo, C., and Nicolini, M.: Climatology of the low-level jet east of the Andes as derived from the NCEP-NCAR reanalyses: characteristics and temporal variability, *J. Climate*, 17, 2261–2280, 2004. 10637
- Mass, C.: Nowcasting: The promise of new technologies of communication, modeling, and observation, *B. Am. Meteorol. Soc.*, 93, 797–809, 2012. 10637
- 5 Mueller, C., Saxen, T., Roberts, R., Wilson, J., Betancourt, T., Dettling, S., Oien, N., and Yee, J.: NCAR auto-nowcast system, *Weather Forecast.*, 18, 545–561, 2003. 10637, 10639
- Pasero, E. and Moniaci, W.: Artificial neural networks for meteorological nowcast, in: *Computational Intelligence for Measurement Systems and Applications*, CIMSA, IEEE International Conference on, Boston, MA, USA, 14–16 July 2004, IEEE, 36–39, 2004. 10640
- 10 Pasini, A., Pelino, V., and Potestà, S.: A neural network model for visibility nowcasting from surface observations: Results and sensitivity to physical input variables, *J. Geophys. Res.-Atmos.*, 106, 14951–14959, 2001. 10640
- Solow, A. R.: On testing for change in extreme events, in: *Weather and Climate Extremes*, Springer, the Netherlands, 341–349, 1999. 10637
- 15 Specht, D. F.: Probabilistic neural networks, *Neural networks*, 3, 109–118, 1990. 10642
- Specht, D. F.: The general regression neural network—rediscovered, *Neural Networks*, 2, 568–576, 1991. 10642
- Teixeira, M. S. and Satyamurty, P.: Dynamical and synoptic characteristics of heavy rainfall episodes in southern Brazil, *Mon. Weather Rev.*, 135, 598–617, 2007. 10637
- 20 Wilks, D. S.: *Statistical Methods in the Atmospheric Sciences: An Introduction*, vol. 59 of International Geophysics Series, Academic Press, London, UK, 255–269, 2006. 10643

10652

**Table 1.** Information from four time series. The lightning time series is the only one whose data period differs from the others. It covers a period from 1 January 2007 to 31 December of 2009. This is not important, since it is used only for validation.

Time series	Frequency and data period	Primary <sup>3</sup> Variables total number: 21	Derived <sup>3</sup> Variables total number: 36	Data percentage data used for SNM training	Data percentage data used for SNM validation	Validation variables	Output variable
Predictors purpose: characterization of atmospheric conditions							
METAR (data are from SBGL, SBSC, SBJR, SBAF and SBRJ)	Hourly from 1 Jan 1997 to 31 Dec 2008	Data-time, wind direction, wind speed, visibility, current weather (represented by 4 classes, see Table 2); cloud layers, temperature, dew point, and atmospheric pressure	Julian day atmospheric pressure (AP) and temperature (AT) for the three previous hours, i.e., $AP_{(t-1h)}$ and $AT_{(t-1h)}$ , $AP_{(t-2h)}$ and $AT_{(t-2h)}$ , and $AP_{(t-3h)}$ and $AT_{(t-3h)}$	70 %	30 %	Class 3 as in Table 2	Rain Rate (RR) <sup>2</sup> = Yes or No (Yes = class 3) or (No = class 0, 1, or 2)
TEMP (data are from SBGL)	Daily at 00:00 and 12:00 UTC from 1 Jan 1997 to 31 Dec 2008	Atmospheric profile of temperature and humidity at 1000, 850, 700 and 500 hPa	(a) three instability indices (K, TT and LR) <sup>1</sup> , (b) potential temperature, vapor pressure, saturation of vapor pressure, zonal, and meridional wind components at 1000, 850, 700 and 500 hPa			–	
Rain Rate (RR) h <sup>-1</sup> (data are from the 29 rain gauges)	Every 15 min from 1 Jan 1997 to 31 Dec 2008	RR for 1 h	(a) RR <sup>2</sup> (classified as null, light, moderate, and heavy), and (b) RR trend for the previous three hours (i.e., $RR_{(t-1h)}$ , $RR_{(t-2h)}$ , and $RR_{(t-3h)}$ )			RR <sup>2</sup> (classified as null, light, moderate, and heavy, corresponding to class 0, 1, 2, and 3, as in Table 2)	
Lightning <sup>4</sup> inside a radius of 50 km centered at SBGL	Varies	–	–	–	100	1 (lightning) or 0 (no lightning)	

<sup>1</sup> K-index (K) =  $(T_{850} - T_{500}) + T_{d850} - (T_{700} - T_{d700})$ , where T and T<sub>d</sub> represent temperature and dew point, respectively, in °C, and T is the given atmospheric pressure in hPa. Total Totals (TT) =  $T_{850} + T_{d850} - 2T_{500}$  and Lapse Rate (LR), represented by  $LR \approx 1000/(500 - T_{500}) / (GPH_{500} - GPH_{700})$ , where GPH means the geopotential height.  
<sup>2</sup> Rain Rate (RR) h<sup>-1</sup>, as null (class zero), light (class one), moderate (class two), and heavy (class three) for RR = insignificant,  $0 \leq RR \leq 2.4$ ,  $2.4 < RR \leq 9.9$ , and  $RR > 9.9 \text{ mm h}^{-1}$ .  
<sup>3</sup> Primary variables are directly extracted from METAR, TEMP, and RR time series, and derived variables are calculated using primary variables.  
<sup>4</sup> Lightning data is only used for SNM validation.

10653

**Table 2.** Weather condition classification in METAR and attributed SNM classes.

Class	METAR code	Weather condition	Class	METAR code	Weather condition
0	H	haze	2	R	moderate rain
0	K	smog	2	RF	moderate rain with fog
0	F	fog	3	R+	heavy rain
0	L–	light drizzle	3	R+ F	heavy rain with fog
0	L– F	light drizzle with fog	3	RW	showers
0	L	moderate drizzle	3	RW+	heavy showers
0	LF	moderate drizzle with fog	3	T	thunderstorms
0	L	heavy drizzle	3	TL	thunderstorms with light drizzle
1	R–	light rain	3	TRW–	thunderstorms with showers
1	R– H	light rain with haze	3	TRW	thunderstorms with moderate showers
1	R– F	light rain with fog	3	TRW+	thunderstorms with heavy showers

10654





**Figure 1.** This is a satellite photo of the Rio de Janeiro metropolitan region. The yellow triangles and red squares represent the twenty-nine rain gauges and five meteorological stations (or airports), respectively.

10657

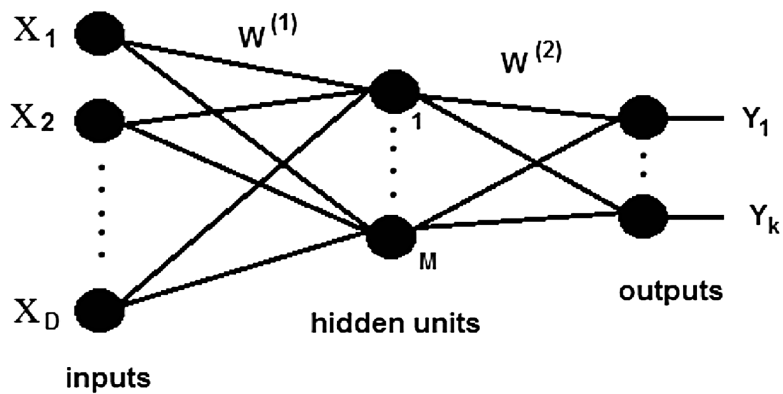


**Figure 2.** An example of a neural network diagram.

10658

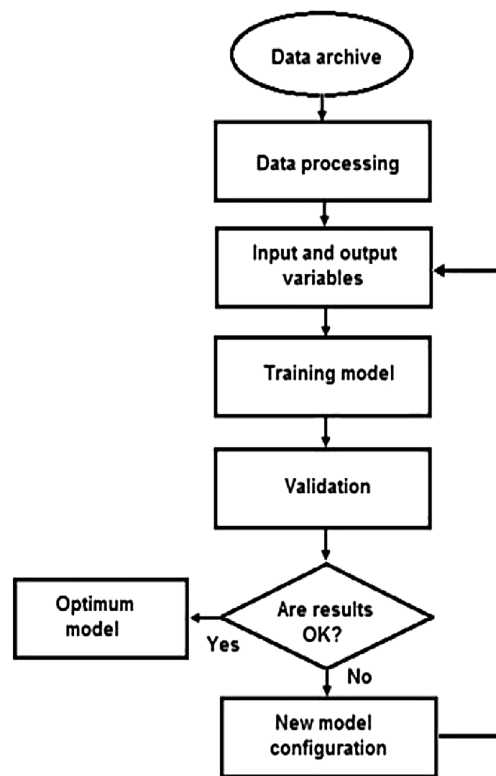


Figure 3. Self-Nowcast Model flowchart.

10659

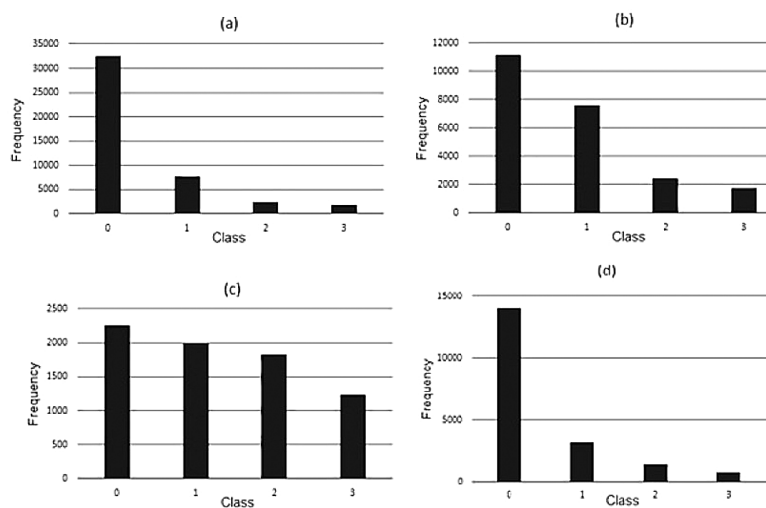
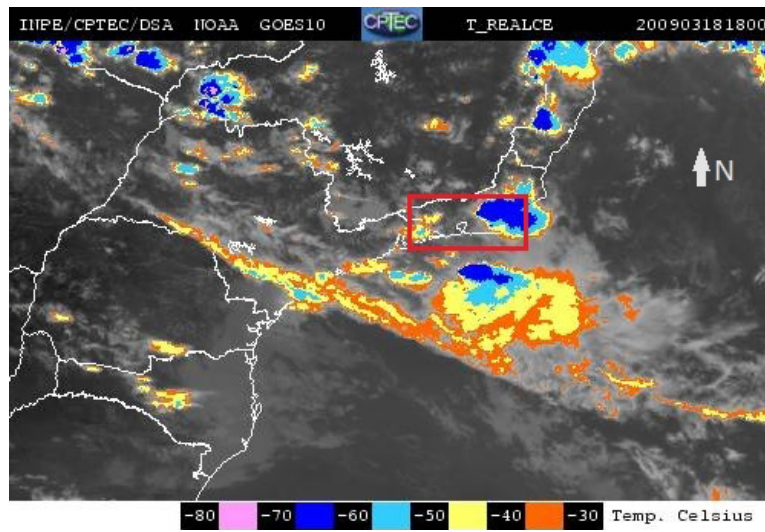


Figure 4. Histograms of frequency accordingly to four event classes: (a) represents 70 % of the original training data set, whose distribution for meteorological recordings for classes zero, one, two, and three are 32 428, 7564, 2412, and 1219, respectively; (b) and (c) similarly present the initial distribution for meteorological recordings for the third and optimum trainings; (d) represents 30 % of the original data set used for SNM validation.

10660



**Figure 5.** GOES-10 (channel 4) that represents the synoptic weather situation at 18:00 (LT) on 18 March 2009, where the top convective cloud temperatures are categorized by a temperature range from  $-30$  to  $-80^{\circ}\text{C}$ . The red box roughly represents the study region.